Comparative Effects of Ibandronate and Paclitaxel on Immunocompetent Bone Metastasis Model

Yoon-Sok Chung[1], Ho Chul Kang[2], and Taeyong Lee[2]

[1]Department of Endocrinology & Metabolism, Ajou University School of Medicine, Suwon;
[2]Department of Medical Biotechnology, Dongguk University, Seoul, Korea.

Purpose: Bone metastasis invariably increases morbidity and mortality. This study compares the effects of ibandronate and paclitaxel on bone structure and its mechanical properties and biochemical turnover in resorption markers using an immunocompetent Walker 256-Sprague-Dawley model, which was subjected to tumor-induced osteolysis.

Materials and Methods: Seventy rats were divided equally into 4 groups: 1) sham group (SHAM), 2) tumor group (CANC), 3) ibandronate treated group (IBAN), and 4) paclitaxel treated group (PAC). Morphological indices [bone volume fraction (BV/TV), trabecular number (Tb.N), trabecular thickness (Tb.Th), trabecular separation (Tb.Sp)] and mechanical properties (failure load, stiffness) were evaluated after thirty days of treatment period. Bone resorption rate was analysed using serum deoxypyridinoline (Dpd) concentrations.

Results: Morphological indices showed that ibandronate (anti-resorptive drug) had a better effect in treating tumor-induced architectural changes in bone than paclitaxel (chemotherapeutic drug). The deterioration in bone architecture was reflected in the biomechanical properties of bone as studied with decreased failure load (F_x) and stiffness (S) of the bone on the 30th day post-surgery. Dpd concentrations were significantly lower in the IBAN group, indicating successful inhibition of bone resorption and destruction.

Conclusion: Ibandronate was found to be as effective as higher doses of paclitaxel in maintaining stiffness of bone. Paclitaxel treatment did not appear to inhibit osteoclast resorption, which is contrary to earlier *in-vitro* literature. Emphasis should be placed on the use of immunocompetent models for examining drug efficacy since it adequately reflects bone metastasis in clinical scenarios.

Key Words: Tumor-induced osteolysis, immunocompetent rodent model, micro-CT, biomechanical properties

INTRODUCTION

The process of metastasis involves the migration of tumor cells from the primary site to other parts of the body via the blood stream or lymphatic channels. Metastatic tumor cells are able to proliferate and grow in secondary sites by escaping from immune surveillance. Bone tissue is one of the three sites, most preferred for solid tumor metastasis,[1] indicating that the bone microenvironment is compatible with secondary tumor growth. Furthermore, common types of cancer, such as breast, lung and prostate cancers, are more likely to result in bone metastasis than other types of cancer.[1] It is estimated that when breast cancer metastasizes to bone, the relative five-year survival rate falls from 90% to less than 10%, indicating a greater need for further investigations into its mechanisms and treatments.[2]

Bone metastasis affects normal bone remodeling, leading to discrete osteolysis, diffuse osteopenia and osteoblastic lesion.[1] Osteolytic tumors have a detrimental effect on the geometry of the bone and its biomechanical properties, since cancer cells enhance bone resorption.[3] The factors released from bone subsequent to resorption (e.g., TGF-β1) provide positive feedback

to the tumor cells, creating a cycle of decay.[4,5]

There are two main categories of drugs for the treatment of tumor osteolysis, namely anti-cancer and anti-resorptive drugs. Paclitaxel, a taxane, is the most commonly used anti-cancer drug to treat breast cancer.[6-8] Paclitaxel, also known as taxol, acts mainly by stabilizing microtubule assembly through non-covalent interactions with tubulin, resulting in blockage of cell replication in the late G2 mitotic phase of the cell cycle, inhibiting proliferation.[9] Bisphosphonates, on the other hand, are a class of anti-resorptive drugs that reduce bone resorption by inhibiting osteoclast activity. Traditionally, bisphosphonates were used in the treatment of osteoporosis, Paget's disease, and other bone metabolic diseases.[10-12] More recently, researchers have established the efficacy of bisphosphonates in the treatment of bone metastases.[5,13-16] In particular, ibandronate, a third generation nitrogen-containing bisphosphonate, has been shown to have the capability to prevent tumor-induced osteolysis and hypercalcemia of malignancy[10,17,18] by inhibiting osteoclast activity. In spite of zoledronic acid being a prominent choice in recent studies as a more potent source of bisphosphonate, ibandronate was chosen for this study, because zoledronic acid is much more likely to cause renal tubule injury, leaving ibandronate an attractive viable option for patients.[19,20]

Most animal models, which have been developed to study bone metastasis are that of immuno-compromised animals,[21-24] which might not adequately represent events in bone metastasis, since the interactions between the immune system, tumor cells and the bone environment are not entirely preserved. Moreover, the treatment response of chemotherapeutic (paclitaxel) and anti-resorptive (ibandronate) drugs on bones affected by osteolytic tumors has not yet been thoroughly studied with the use of an immunocompetent animal model. Therefore, the objective of this study is to investigate the micro-architectural and mechanical effects of chemotherapeutic (paclitaxel) and anti-resorptive (ibandronate) treatments, together with an analysis of bone resorption markers [deoxypyridinoline (Dpd)] in a tumor metastatic immunocompetent animal model. It is hypothesized that anti-resorptive drugs (ibandronate) are as effective as high doses of chemotherapeutic (paclitaxel) drug in preserving bone micro-architectural and mechanical properties.

MATERIALS AND METHODS

Cell culture

Walker carcinoma 256 (W256) malignant rat breast cancer cells (ATCC, CCL-38 LLC-WRC 256 cells, Manassas, VA, USA) were cultured in M199 culture media (Sigma-Aldrich, St. Louis, MO, USA) with 5% horse serum (Sigma-Aldrich, St. Louis, MO, USA). The cells were maintained in a 5% carbon dioxide incubator at 37°C. On the day of surgery, cells were harvested and counted using a hemocytometer. Approximately 2.5×10^6 cells were suspended in 0.5 mL of saline in every surgery and used to develop the osteolytic tumor rat model.

Animals

Seventy female Sprague-Dawley (SD) rats, aged 10–12 weeks, were housed at the Laboratory Animal Centre in a light-controlled environment (12 h light-dark cycle) under standard temperature (23±1°C). They were fed with standard rodent chow and water ad libitum. The rats were randomly divided into four groups (SHAM, CANC, IBAN, and PAC). SHAM (n=16) was the control group while CANC (n=18) was used to observe the effect and progression of tumor growth. IBAN (n=18) and PAC (n=18) were administered with ibandronate and paclitaxel, respectively. All rats from the CANC, IBAN, and PAC groups had Walker Carcinoma 256 cells injected into their right femoral medullary canal via a drill hole made through the intercondylar notch to develop the osteolytic tumor.[18] Rats from the SHAM group (n=16) also underwent similar surgical procedure, but saline was injected instead of cancer cells.

The IBAN group rats were given a subcutaneous administration of ibandronate (Bondronat®, Roche Diagnostics GmbH, Mannheim, Germany) at a dosage of 250 μg/kg of rat,[18] once every ten days, starting from the day of the surgery. The increased inhibition of osteoclast resorption, coupled with ongoing bone formation, results in preservation of bone mass and architecture. However, exceeding a certain threshold of drug dosage (in this case 10 μg P/kg) results in decreased bone formation.[25] This is why the mid value of the prescribed range (0.1<1<10 μg P/kg/day) was chosen. Paclitaxel (Anzatax®, Mayne Pharma Pte Ltd., Salisbury South, Australia) was administered intravenously at a dosage of 10 mg/kg of rat via the lateral tail vein of the PAC group rats, once every 10 days from the day of surgery.[7] The CANC and SHAM group rats were given placebo treatment. Six (IBAN, PAC, and CANC) and four

Sham operated (SHAM)	Osteolytic response
A	B

Fig. 1. X-ray showing (A) sham operated left femur of SHAM group and (B) osteolytic lesions (white arrows) in left femur of CANC group.[26]

(SHAM) rats from each group were euthanized at intervals of 10 days and the femoral bones were harvested. The excised femurs were cleaned such that soft tissue was removed, wrapped in 0.9% saline-soaked gauze and stored in -20°C freezer.

X-ray

X-ray scanning of all rats was performed 10 days after the tumor inoculations by using Kodak DXS 4000 system at 35 kV for 2 minutes. X-ray analysis was performed with radiological scores given as follows: Grade 0 for no radiolucent lesion observed, Grade 1 for minimal but detectable lysis within the canal, Grade 2 for moderate lysis limited to the canal, and Grade 3 for extensive lesions extending into soft tissues.[2,26] In this study, rats with detectable osteolysis were chosen for CANC and treatment (IBAN, PAC) groups. Only rats with osteolytic response (Grade 3 as in Fig. 1B) were utilized since sclerosis (tissue hardening) develops in slow growing or benign osteolytic lesions, in which it appears to limit lesion growth indicating regression of osteolysis.[26]

Micro-computed tomography

Prior to micro-computed tomography (μCT) scanning, the femurs were thawed to room temperature (25°C). The right distal femoral metaphysis was scanned using the SkyScan μCT machine (SkyScan 1172, Konitch, Belgium). The volume of interest (VOI), containing 152 CT slices, was located 6 mm away from the distal intercondylar notch and covered a region of 2 mm of the distal femur metaphysis as shown in Fig. 2A. Resolution of the scans was set at 13.148 μm. An average pixel size of 6 μm was used for scanning. These images were then analyzed, and four morphological indices, namely bone volume faction (BV/TV), trabecular number (Tb.N), trabecular separation (Tb.Sp) and trabecular thickness (Tb.Th), were obtained for micro-architectural analysis.[3]

Mechanical testing

The failure load (F_x) and stiffness (S) of femur specimens were obtained using the three-point bending test (Instron 5848 micro-testing machine, Norwood, MA, USA). Prior to testing, the femurs were thawed in 0.9% saline for about two hours until they reached room temperature (−25°C). Femurs were placed posterior side up on supports spanning 15 mm and a stabilizing preload of 10 N was applied at the center of the femur. The specimen was loaded till fracture at a deformation rate of 0.1 mm/s. The data acquisition interval was set to 5 ms. Testing conditions were determined through preliminary experiments.[27,28] The maximum force observed in the load-deformation plot was taken as F_x and the slope of the linear portion of the plot as the S.

Bone turnover marker

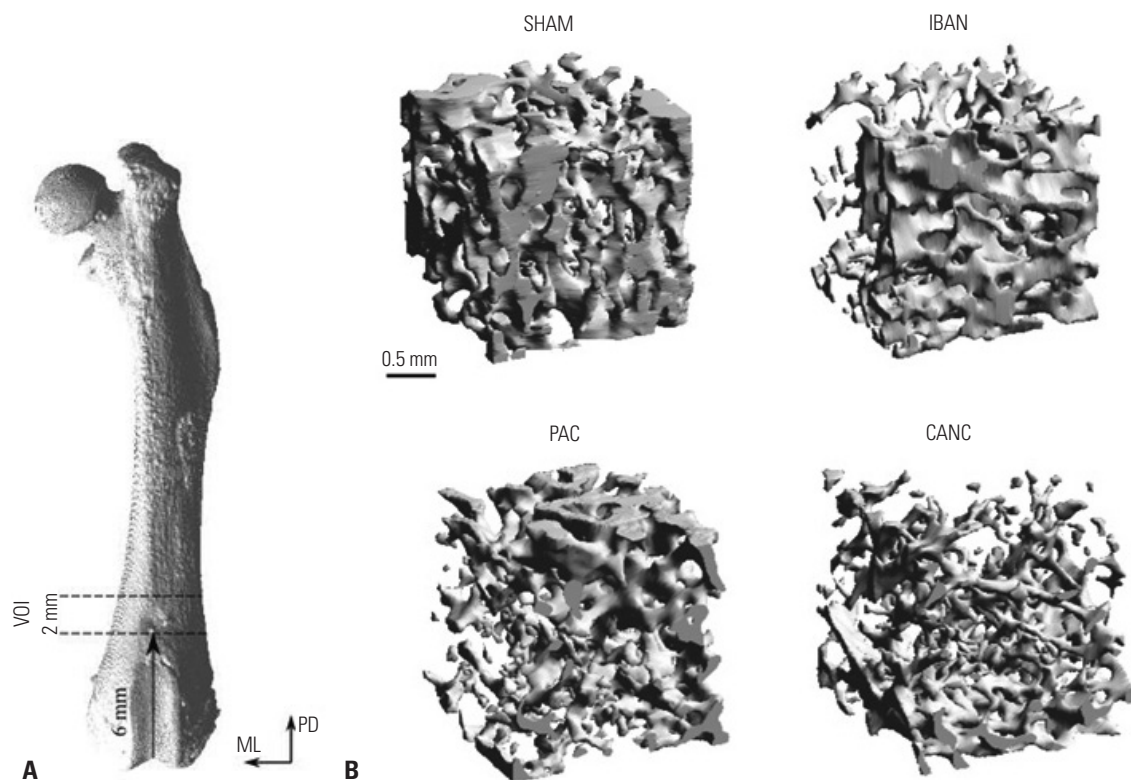Approximately 1 mL of blood was collected from the central tail

Fig. 2. (A) Sprague-Dawley rat femur showing the VOI for micro-CT scanning. (B) Micro-CT image of the distal femurs of SHAM, IBAN, PAC, and CANC groups at 30 days. VOI, volume of interest; ML, medial lateral; PD, proximal distal.

artery of each rat at 0, 10, 20, and 30 days. After standing for an hour, the blood was centrifuged at 4600 rpm for 20 minutes. The serum was then separated and stored at -20°C. The Metra® Total DPD EIA Kit (Mountain View, CA, USA) was used to determine the level of Dpd in serum to assess bone resorption activity.[29]

Statistical analysis

The SPSS 16.0 software (SPSS Inc., Chicago, IL, USA) was used for statistical analysis. Mean and standard deviation of all the variables were reported. One-way ANOVA was performed by time to determine significant differences between different groups at each time point. Similarly, one-way ANOVA test was also performed by respective groups to determine the significant differences of each group over the time period. Bonferroni corrections were used for all the comparisons and the results were considered to be statistically significant when $p < 0.05$.

RESULTS

Morphological analysis

X-ray images of the SHAM and CANC groups are shown in Fig. 1. The cancer induced right femur (Fig. 1B) shows obvious osteolytic, radiolucent lesions (white arrows) unlike the sham operated right femur (Fig. 1A).

μCT images (1.5 mm by 1.5 mm) of distal rat femurs of all the four groups are shown in Fig. 2B. The CANC group exhibited reduced bone mass compared to the SHAM group. On the other hand, the IBAN and PAC groups displayed increased bone mass compared to the CANC group, indicating their efficacy in preventing bone loss.

The changes in BV/TV, Tb.N, Tb.Sp, and Tb.Th of different groups with respect to time are indicated in Fig. 3, respectively. Analysis of the four groups indicated that there were no significant differences in Tb.Th across groups or time. As expected, the SHAM group revealed no significant variation in morpho-
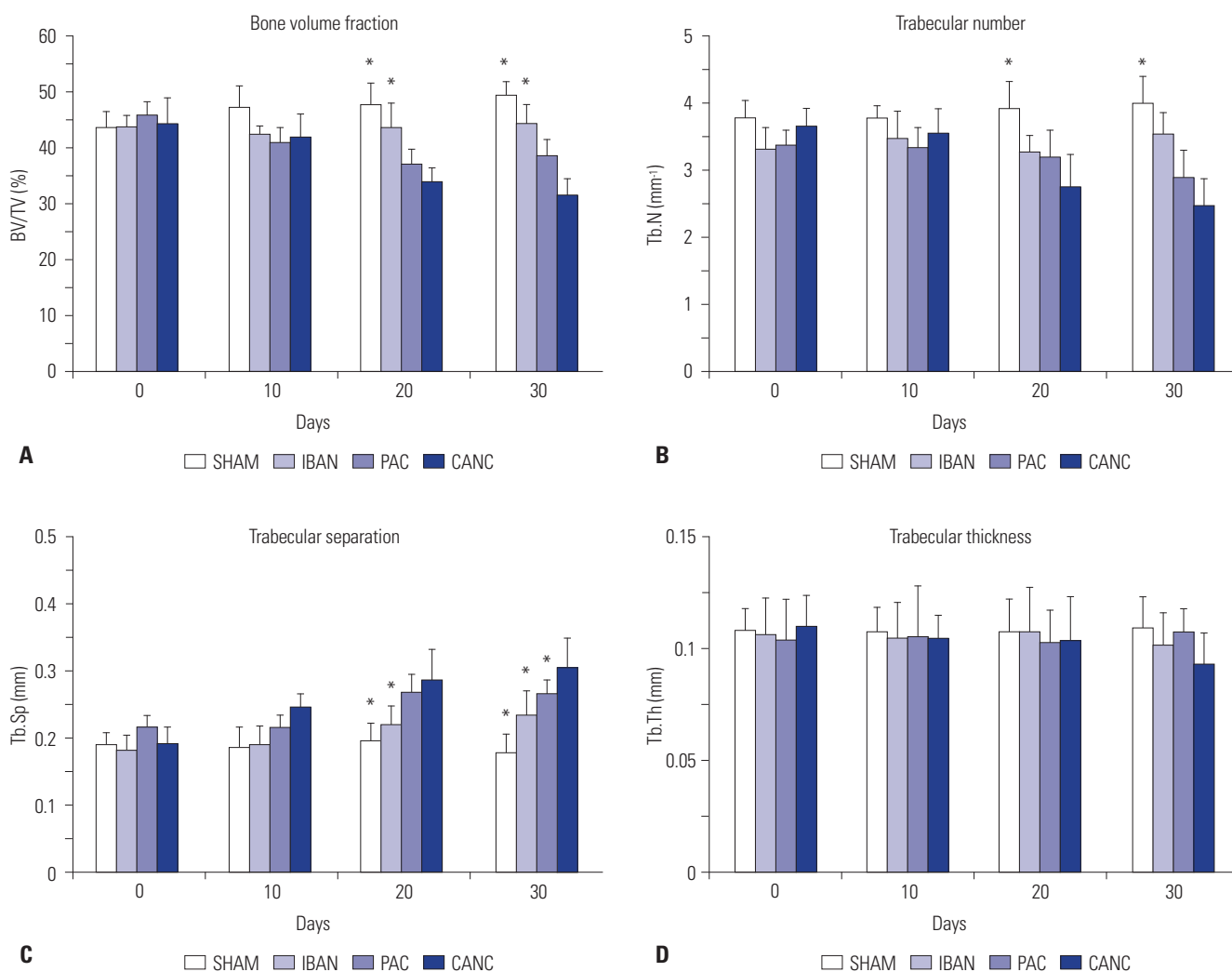

Fig. 3. Changes in morphological parameters of 4 different groups (SHAM, IBAN, PAC, and CANC) at 0, 10, 20, and 30 days using micro-CT. (A) Bone volume ratio, bone volume fraction (BV/TV). (B) Trabecular number (Tb.N). (C) Trabecular separation (Tb.Sp). (D) Trabecular thickness (Tb.Th). *Significance ($p < 0.05$) with respect to CANC group by one way ANOVA with Bonferroni corrections.

logical indices across the entire duration of the experiment.

However, 20 days post-surgery, CANC group showed a significant decrease in the BV/TV and Tb.N, while the Tb.Sp showed a significant increase as compared to the SHAM group. By the 30th day post-surgery, BV/TV and Tb.N of the CANC group were lower than those of the SHAM group by 36% ($p<$0.001) and 38% ($p=0.007$), respectively. Furthermore, Tb.Sp of the CANC group was 92% higher than that of the SHAM group ($p<0.001$). These results confirm the successful induction of osteolytic tumors in the CANC group rats.

Starting from 20 days post-surgery, IBAN group rats showed significant variation in the morphological indices, i.e., the IBAN group was 40% ($p=0.04$) higher than CANC in BV/TV and 32% lower in Tb.Sp ($p<0.001$). However, Tb.N did not vary significantly between the two groups. Also, bone morphological indices of the IBAN group were not significantly different from those of the SHAM group.

The PAC group did not show significant differences in the BV/TV or Tb.N as compared to the CANC group at any point in the experiment. However, at the 30th day post-surgery, Tb.Sp of the PAC group was 22% lower than that of the CANC group ($p=0.036$). Unlike the IBAN group, the PAC group also showed significant differences in the BV/TV, Tb.N, and Tb.Sp, compared to the SHAM group.

Mechanical testing

F_x and S of different groups of rats with respect to time are shown in Fig. 4, respectively. The SHAM group showed no significant differences in the F_x and S of the bone over time. However, the CANC group showed significant decrease in both F_x and S. The decrease in F_x gained significance by the 30th day post-surgery (13.3%, $p<0.03$) and the decrease in S gained significance by the 20th day post-surgery (12.5%, $p<0.001$) as compared to SHAM.

The F_x values for both PAC and IBAN groups were similar and significantly higher than those of CANC group. Thirty days after surgery, the IBAN group had a 7.7% higher S value than CANC group ($p=0.036$) and 6.9% lower than SHAM group ($p=0.041$). There was no significant difference in the S values between the PAC and IBAN groups.

Bone turnover marker

The serum Dpd concentration for each rat was normalized against the reading on day zero, as shown in Table 1. The Dpd concentration of the CANC group increased by 31% after 10 days, 27% after 20 days, and 11.8% after 30 days, while Dpd concentrations in the SHAM group showed no significant variation.

The Dpd concentration of the IBAN group decreased by 37.9% after 10 days, 48.2% after 20 days, and 38.9% after 30 days, indicating that ibandronate treatment is effective in de-
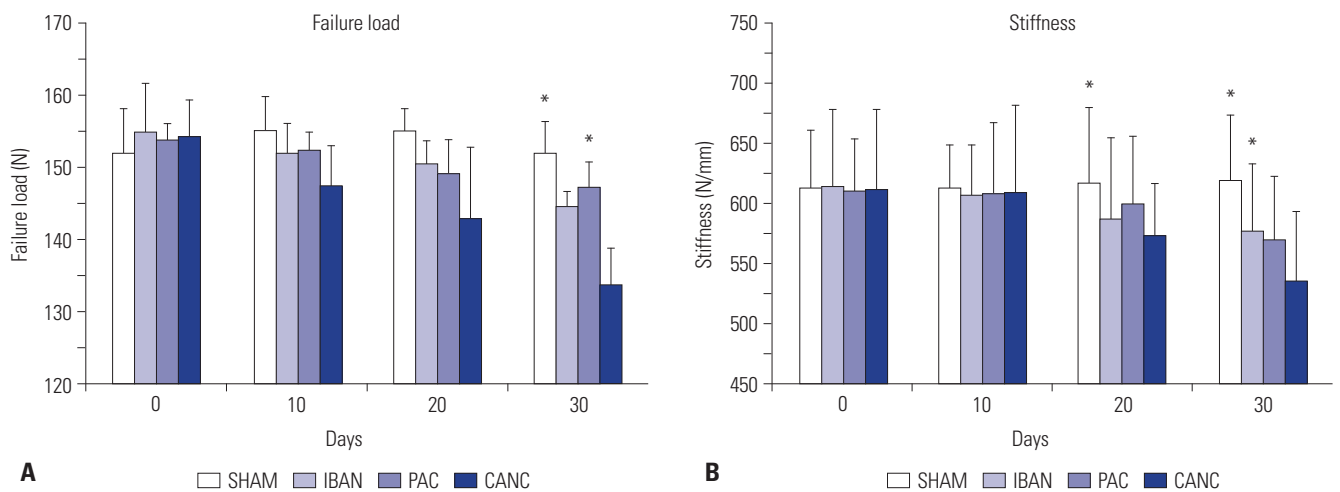

Fig. 4. Changes in (A) failure load (F_x) and (B) stiffness (S) of 4 different groups (SHAM, IBAN, PAC, and CANC) at 0, 10, 20, and 30 days. *Significance ($p<0.05$) with respect to CANC group by one way ANOVA with Bonferroni corrections.

Table 1. Serum Total Dpd Concentration of Four Different Animal Groups (SHAM, IBAN, PAC, and CANC)

Parameter	Group	Time from surgery (days)			
		0	10	20	30
Dpd (normalized)	SHAM	1.00	1.03	0.92	0.88
	IBAN	1.00	0.62*	0.52*	0.61*
	PAC	1.00	1.19	1.15	1.28
	CANC	1.00	1.31*	1.27*	1.18*

*$p<0.05$ as compared to the 0 day data.

creasing bone resorption. The PAC group did not show a clear trend in serum Dpd levels. This implies that there was no decrease in bone resorption activity for paclitaxel treated bones.

DISCUSSION

This study investigated the effects of tumor-induced osteolysis in an immunocompetent rodent model involving the inoculation of W256 carcinoma cells in SD rat femur. The efficacy of chemotherapeutic (paclitaxel) and anti-resorptive (ibandronate) treatment in overcoming the effects of metastasis was analyzed in terms of bone structural properties, biomechanical properties and biochemical marker analysis.

It has been reported that granulocytes can play an important role in immune response against initial stages of Walker 256 carcinoma development in SD rats, potentially affecting the characteristics of the tumor and are subsequently established in the host environment.[30] The varied tumor responses observed in different host bodies subsequent to the inoculation of tumor cells could be a consequence of host body immune response. Four responses were noted; osteolytic, mixed (osteolytic with osteosclerotic signs), osteosclerotic healing flare and no response. Only rats with osteolytic responses were utilized for the cancer (CANC) and treatment (IBAN, PAC) groups in this study. It is an observation, although not unexpected, which was not widely reported in earlier studies of immunocompetent models[31] including the study conducted by Kurth and Müller[3] It could be due to a pre-selection of cell types prior to surgery i.e., induction of ascites in host bodies[23] or soft agar growth of tumor cells before surgery.[3] Nonetheless, successful adoption of an immunocompetent model imitates the actual environment in tumor osteolysis and helps clarify the effects of drugs on bone metastasis in a clinical setting.

Successful osteolytic tumor induction in this model had a harmful effect on bone architecture, as seen from the significant drop in BV/TV and Tb.N and rise in Tb.Sp in the CANC group in 20 days after surgery. This deterioration in bone architecture[32-34] was reflected in the biomechanical properties of bone, as evidenced from the decreased F_x and S of the bone on the 30th day post-surgery. The total serum Dpd concentration also showed an increase after tumor induction. Based on these results and μCT images, it is reasonable to conclude that tumor growth had been induced in the femoral bone in the osteolytic tumor rat models, causing accelerated bone resorption and micro-architectural deterioration, further leading to the loss of biomechanical competence in bone.

Previous studies showed that Tb.Th varied significantly after tumor induction.[3,18] However, we did not observe statistically significant differences in Tb.Th between different groups or at different time periods. It is possible that Tb.Th is decreasing and the trend is masked by the disconnection of thinner trabeculae.

Morphological indices showed that ibandronate (anti-resorptive drug) had a better effect in treating tumor-induced architectural changes in bone than paclitaxel (chemotherapeutic drug). On the 30th day post-surgery, the BV/TV of IBAN was 40% higher than that of the CANC group, whereas a significant difference was not observed in the PAC group. This concurs with the study conducted by Strube, et al.,[35] where MDA-MB-231 (SA) breast cancer to bone metastasis mouse model treated with paclitaxel (9 mg/kg i.p. once daily, 13–17 days) failed to show any significant change in BV/TV, compared to the vehicle-treated group. Similarly, Tb.Sp of the IBAN group was found to be 32% lower than that of the CANC group as compared to 22% of the PAC group. This trend indicates that ibandronate is more effective than paclitaxel in maintaining the structural properties of bone and preventing tumor-induced bone architectural changes. These experimental observations can be related to the mechanism of action of individual drugs, i.e., ibandronate directly inhibits osteoclast resorption and promotes osteoclast apoptosis at a later time[16,36] while paclitaxel stabilizes microtubule formation, arresting tumor cell division at the mitotic boundary,[37] thereby indirectly affecting the degree of bone destruction induced by tumor cells.

Also, Dpd concentrations were significantly lower in the IBAN group, indicating successful inhibition of bone resorption and destruction. However, paclitaxel appeared to have no effect on Dpd concentration, and consequently, minimal effect on osteoclast resorption. Earlier in vitro studies have shown dose-related inhibition effects of paclitaxel on osteoclastic resorption.[35,38] However, paclitaxel is now shown to have negligible in-vivo effect on bone resorption even at 10 mg/kg, which is the maximum dosage that could be safely administered to rodent models.[7,37,39,40]

Apart from inhibiting osteoclast resorption, ibandronate treatment may allow more time for secondary mineralization,[41] which aids in increasing bone mineral density,[10,42] thus preserving bone S. There are also reports of in vitro and in vivo evidence of bisphosphonates having anti-tumor effects[25,41-48] which might aid further preservation of bone strength and integrity. Therefore, the finding that ibandronate (250 μg/kg) has similar efficacy in maintaining bone mechanical properties to high doses of paclitaxel (10 mg/kg) is surprising since efficacy of ibandronate in bone preservation is well-established. Paclitaxel, on the other hand, is shown to have negligible effect on in vivo bone resorption, nevertheless, it preserves bone mechanical properties, comparable to ibandronate.

Before postulating that paclitaxel may have a direct effect on bone through other mechanisms that do not involve inhibition of bone resorption, bone biopsy and subsequent histomorphometric analysis are required to derive explicit conclusions on the effect of paclitaxel on bone remodeling.[35,38] Histomorphometric analysis will also be useful in determining

the extent to which ibandronate affects tumor proliferation and growth in the intramedullary space. Halvorson, et al.[36] reported that ibandronate induced extensive tumor cell necrosis in C3H/HeJ mice bearing osteolytic 2472 sarcoma cells. Earlier *in vitro* studies have also suggested that bisphosphonates have an influence on neovascularization.[36] The specific mechanisms by which bisphosphonates can influence the growth of tumor metastasis and its viability are currently unclear and developing an understanding is an important objective of future research in the field of drug therapeutics.

In summary, an immunocompetent model was adopted where Walker 256 carcinoma cells provoked a localized increase in bone resorption, resulting in bone loss. Ibandronate was found to be as effective as high doses of paclitaxel in maintaining S of bone. Paclitaxel treatment did not appear to inhibit osteoclast resorption, which is contrary to earlier *in vitro* literature. The immune system also plays a plausible role in the selection of tumor cells as seen from the varied responses of the heterogeneous W256 carcinoma cells in the different host bodies. Emphasis should be placed on the use of immunocompetent models for examining drug efficacy for bone metastasis since it adequately reflects bone metastasis in clinical scenarios.

ACKNOWLEDGEMENTS

REFERENCES

1. Mundy GR. Mechanisms of bone metastasis. Cancer 1997;80(8 Suppl):1546-56.
2. Bussard KM, Mastro AM. Ex-vivo analysis of the bone microenvironment in bone metastatic breast cancer. J Mammary Gland Biol Neoplasiam 2009;14:387-95.
3. Kurth AA, Müller R. The effect of an osteolytic tumor on the three-dimensional trabecular bone morphology in an animal model. Skeletal Radiol 2001;30:94-8.
4. Alvarez E, Westmore M, Galvin RJ, Clapp CL, Considine EL, Smith SJ, et al. Properties of bisphosphonates in the 13762 rat mammary carcinoma model of tumor-induced bone resorption. Clin Cancer Res 2003;9:5705-13.
5. Bauss F, Body JJ. Ibandronate in metastatic bone disease: a review of preclinical data. Anticancer Drugs 2005;16:107-18.
6. Peltier S, Oger JM, Lagarce F, Couet W, Benoît JP. Enhanced oral paclitaxel bioavailability after administration of paclitaxel-loaded lipid nanocapsules. Pharm Res 2006;23:1243-50.
7. Shord SS, Camp JR. Intravenous administration of paclitaxel in Sprague-Dawley rats: what is a safe dose? Biopharm Drug Dispos 2006;27:191-6.
8. Stearns ME, Wang M. Effects of alendronate and taxol on PC-3 ML cell bone metastases in SCID mice. Invasion Metastasis 1996; 16:116-31.
9. Heldman AW, Cheng L, Jenkins GM, Heller PF, Kim DW, Ware M Jr, et al. Paclitaxel stent coating inhibits neointimal hyperplasia at 4 weeks in a porcine model of coronary restenosis. Circulation 2001;103:2289-95.
10. Lalla S, Hothorn LA, Haag N, Bader R, Bauss F. Lifelong administration of high doses of ibandronate increases bone mass and maintains bone quality of lumbar vertebrae in rats. Osteoporos Int 1998;8:97-103.
11. Russell RG, Watts NB, Ebetino FH, Rogers MJ. Mechanisms of action of bisphosphonates: similarities and differences and their potential influence on clinical efficacy. Osteoporos Int 2008;19: 733-59.
12. Muthukumaran P, Lim CT, Lee T. Estradiol influences the mechanical properties of human fetal osteoblasts through cytoskeletal changes. Biochem Biophys Res Commun 2012;423:503-8.
13. Coleman RE. Adjuvant bisphosphonates in breast cancer: are we witnessing the emergence of a new therapeutic strategy? Eur J Cancer 2009;45:1909-15.
14. Diel IJ. Antitumour effects of bisphosphonates: first evidence and possible mechanisms. Drugs 2000;59:391-9.
15. Hall DG, Stoica G. Effect of the bisphosphonate risedronate on bone metastases in a rat mammary adenocarcinoma model system. J Bone Miner Res 1994;9:221-30.
16. Russell RG. Ibandronate: pharmacology and preclinical studies. Bone 2006;38(4 Suppl 1):S7-12.
17. Kurth AA, Kim SZ, Sedlmeyer I, Bauss F, Shea M. Ibandronate treatment decreases the effects of tumor-associated lesions on bone density and strength in the rat. Bone 2002;30:300-6.
18. Kurth AA, Kim SZ, Shea M, Bauss F, Hayes WC, Müller R. Preventative ibandronate treatment has the most beneficial effect on the microstructure of bone in experimental tumor osteolysis. J Bone Miner Metab 2007;25:86-92.
19. Fan TM. Intravenous aminobisphosphonates for managing complications of malignant osteolysis in companion animals. Top Companion Anim Med 2009;24:151-6.
20. Yang X, Chan YH, Muthukumaran P, Dasde S, Teoh SH, Lee T. Ibandronate does not reduce the anabolic effects of PTH in ovariectomized rat tibiae: a microarchitectural and mechanical study. Bone 2011;48:1154-63.
21. Arrington SA, Schoonmaker JE, Damron TA, Mann KA, Allen MJ. Temporal changes in bone mass and mechanical properties in a murine model of tumor osteolysis. Bone 2006;38:359-67.
22. Chanda D, Isayeva T, Kumar S, Siegal GP, Szafran AA, Zinn KR, et al. Systemic osteoprotegerin gene therapy restores tumor-induced bone loss in a therapeutic model of breast cancer bone metastasis. Mol Ther 2008;16:871-8.
23. Mann KA, Lee J, Arrington SA, Damron TA, Allen MJ. Predicting distal femur bone strength in a murine model of tumor osteolysis. Clin Orthop Relat Res 2008;466:1271-8.
24. Neudert M, Fischer C, Krempien B, Bauss F, Seibel MJ. Site-specific human breast cancer (MDA-MB-231) metastases in nude rats: model characterisation and in vivo effects of ibandronate on tumour growth. Int J Cancer 2003;107:468-77.
25. Fleisch H. The bisphosphonate ibandronate, given daily as well as discontinuously, decreases bone resorption and increases calcium retention as assessed by 45Ca kinetics in the intact rat. Osteoporos Int 1996;6:166-70.
26. Chen X, Goh JC, Teoh SH, De SD, Soong R, Lee T. Localized sclerotic bone response demonstrated reduced nanomechanical

creep properties. J Mech Behav Biomed Mater 2013;17:198-208.

27. Yang X, Chan YH, Muthukumaran P, Lee T. Morphological and mechanical changes in ovariectomized rat tibia with treatments of ibandronate and parathyroid hormone. Osteoporosis 2010;8: 255-65.

28. Yang X, Muthukumaran P, Lee T. Effect of ibandronate and hPTH on the viscoelastic response of ovariectomized rat femur. Osteoporosis 2011;9:222-30.

29. Allen MJ. Biochemical markers of bone metabolism in animals: uses and limitations. Vet Clin Pathol 2003;32:101-13.

30. Jaganjac M, Poljak-Blazi M, Zarkovic K, Schaur RJ, Zarkovic N. The involvement of granulocytes in spontaneous regression of Walker 256 carcinoma. Cancer Lett 2008;260:180-6.

31. Jung A, Bornand J, Mermillod B, Edouard C, Meunier PJ. Inhibition by diphosphonates of bone resorption induced by the Walker tumor of the rat. Cancer Res 1984;44:3007-11.

32. Lee T. Predicting failure load of the femur with simulated osteolytic defects using noninvasive imaging technique in a simplified load case. Ann Biomed Eng 2007;35:642-50.

33. Lee T, Pereira BP, Chung YS, Oh HJ, Choi JB, Lim D, et al. Novel approach of predicting fracture load in the human proximal femur using non-invasive QCT imaging technique. Ann Biomed Eng 2009;37:966-75.

34. Lee T, Choi JB, Schafer BW, Segars WP, Eckstein F, Kuhn V, et al. Assessing the susceptibility to local buckling at the femoral neck cortex to age-related bone loss. Ann Biomed Eng 2009;37:1910-20.

35. Strube A, Hoffmann J, Stepina E, Hauff P, Klar U, Käkönen SM. Sagopilone inhibits breast cancer bone metastasis and bone destruction due to simultaneous inhibition of both tumor growth and bone resorption. Clin Cancer Res 2009;15:3751-9.

36. Halvorson KG, Sevcik MA, Ghilardi JR, Sullivan LJ, Koewler NJ, Bauss F, et al. Intravenous ibandronate rapidly reduces pain, neurochemical indices of central sensitization, tumor burden, and skeletal destruction in a mouse model of bone cancer. J Pain Symptom Manage 2008;36:289-303.

37. Steed H, Sawyer MB. Pharmacology, pharmacokinetics and pharmacogenomics of paclitaxel. Pharmacogenomics 2007;8:803-15.

38. Hall TJ, Jeker H, Schaueblin M. Taxol inhibits osteoclastic bone resorption. Calcif Tissue Int 1995;57:463-5.

39. Ermolaeva LA, Dubskaya TY, Fomina TI, Vetoshkina TV, Gol'dberg VE. Toxic effect of an antitumor drug paclitaxel on morphofunctional characteristics of the liver in rats. Bull Exp Biol Med 2008; 145:263-5.

40. Tarumi W, Suzuki N, Takahashi N, Kobayashi Y, Kiguchi K, Sato K, et al. Ovarian toxicity of paclitaxel and effect on fertility in the rat. J Obstet Gynaecol Res 2009;35:414-20.

41. Brennan TC, Rizzoli R, Ammann P. Selective modification of bone quality by PTH, pamidronate, or raloxifene. J Bone Miner Res 2009;24:800-8.

42. Chavassieux PM, Arlot ME, Reda C, Wei L, Yates AJ, Meunier PJ. Histomorphometric assessment of the long-term effects of alendronate on bone quality and remodeling in patients with osteoporosis. J Clin Invest 1997;100:1475-80.

43. Boissier S, Ferreras M, Peyruchaud O, Magnetto S, Ebetino FH, Colombel M, et al. Bisphosphonates inhibit breast and prostate carcinoma cell invasion, an early event in the formation of bone metastases. Cancer Res 2000;60:2949-54.

44. Fromigue O, Lagneaux L, Body JJ. Bisphosphonates induce breast cancer cell death in vitro. J Bone Miner Res 2000;15:2211-21.

45. Ottewell PD, Woodward JK, Lefley DV, Evans CA, Coleman RE, Holen I. Anticancer mechanisms of doxorubicin and zoledronic acid in breast cancer tumor growth in bone. Mol Cancer Ther 2009;8:2821-32.

46. Verdijk R, Franke HR, Wolbers F, Vermes I. Differential effects of bisphosphonates on breast cancer cell lines. Cancer Lett 2007; 246:308-12.

47. Winter MC, Holen I, Coleman RE. Exploring the anti-tumour activity of bisphosphonates in early breast cancer. Cancer Treat Rev 2008;34:453-75.

48. Zheng Y, Zhou H, Brennan K, Blair JM, Modzelewski JR, Seibel MJ, et al. Inhibition of bone resorption, rather than direct cytotoxicity, mediates the anti-tumour actions of ibandronate and osteoprotegerin in a murine model of breast cancer bone metastasis. Bone 2007;40:471-8.